2014-06-13

Phenomenology of Low Probability of Intercept Synthetic Aperture Radar via Frank Codes

Romero, Ric A.; Garren, David A.; Pace, Phillip E.

SPIE

Proc. of SPIE, Volume 9093 909302-1 (2014),
http://hdl.handle.net/10945/48645

Phenomenology of Low Probability of Intercept Synthetic Aperture Radar via Frank Codes

David A. Garren[a], Phillip E. Pace[a], and Ric A. Romero[a]

[a]Department of Electrical and
Computer Engineering, Naval Postgraduate School, Monterey, CA 93943, USA

ABSTRACT

This paper investigates techniques for using low probability of intercept (LPI) modulation techniques for forming synthetic aperture radar (SAR) imagery. This analysis considers a specific waveform type based upon Frank codes in providing for the LPI capability via phase shift keying (PSK) modulation. A correlation receiver that is matched to the transmitted waveform is utilized to generate a set of SAR data. This analysis demonstrates the ability to form SAR images based upon simulated radar measurements collected by a notional radar sensor that has ability to transmit and receive Frank-coded waveforms and to form SAR images based upon the results of a correlation receiver. Spotlight-mode SAR images are generated using the Frank-coded waveforms and their properties are analyzed and discussed.

Keywords: Synthetic aperture radar, Low probability of intercept, Radar imaging, Radar theory

1. INTRODUCTION

This paper investigates methods for using low probability of intercept (LPI) transmission waveforms in order to construct synthetic aperture radar (SAR) imagery. This analysis considers a specific waveform based upon Frank codes, which provides a particular type of a phase shift keying (PSK) modulation. A matched correlation receiver is utilized to generate a set of SAR data for the transmitted Frank-modulated waveforms. The resulting two-dimensional impulse response shape within the SAR image is analyzed in terms of the radar parameters.

The objective of this investigation is to analyze the properties of SAR images formed from a particular LPI modulation based upon the Frank code. This analysis demonstrates the ability to form SAR images based upon simulated radar measurements collected by a notional radar sensor with a capability to transmit and receiver LPI-SAR radar waveforms. The SAR image formation quality and LPI performance corresponding to this PSK waveform is analyzed and discussed.

Giusti and Martorella[3] have used Frequency-Modulated Continuous Wave (FMCW) waveforms, which comprises another type of LPI waveform – to generate Inverse SAR (ISAR) images. The present analysis considers the use of Frank-coded waveforms[?, 2, 7] in order to form SAR images of a stationary scene using spotlight-mode SAR methods. Spotlight-mode SAR is a radar imaging mode[1, 5, 6, 9, 10] which continuously steers the radar mainbeam in the direction of a single fixed point on the ground. This SAR imaging mode can often yield good image resolution, but it has a lower area coverage rate than that of stripmap SAR.

For the initial part of the simulation activity, it is necessary to generate the idealized impulse response of the scene corresponding to the radar sensor aspect and elevation angles for each radar waveform that is transmitted along the radar's synthetic aperture. The result of the ideal correlation processing is obtained by taking the convolution of the complex conjugate of the time-reversed transmitted waveform with the received radar echo from the scene location where the gain of the radar transmission beam is steered for that particular waveform. These idealized radar responses give the effective impulse response of the scene at the particular azimuthal and elevation angles of the radar sensor relative to the scene of interest.

Further author information: (Send correspondence to D.A.G)
D.A.G.: E-mail: dagarren@nps.edu
P.E.P.: E-mail: pepace@nps.edu
R.A.R.: E-mail: rnromero@nps.edu

Algorithms for Synthetic Aperture Radar Imagery XXI, edited by Edmund Zelnio, Frederick D. Garber, Proc. of SPIE
Vol. 9093, 909302 · © 2014 SPIE · CCC code: 0277-786X/14/$18 · doi: 10.1117/12.2048638

In order to obtain an accurate model of the receiver processing, it is useful to employ a set of idealized radar echoes. Each of these simulated idealized radar echoes is convolved with the selected Frank-coded radar waveform for each relevant azimuthal angle and elevation angle along the synthetic aperture. Specifically, the result of this correlation receiver processing is obtained by computing the convolution of the received waveform with the complex conjugate of the time-reversed transmission waveform at the set of measurement angles under interrogation. This correlation processing yields the range profile of the scene corresponding to each transmitted Frank-coded waveform along the synthetic aperture. This correlation processing effectively dispreads the radar echoes that enter the receiver, so that range profiles are extracted from the scene consistent with the sidelobe properties of Frank waveforms. The resulting complex-valued range profiles enable the generation of conventional spotlight-mode SAR imagery of the scene of interest. The properties of the SAR image obtained from the use of Frank-coded waveforms are analyzed and discussed.

The next section defines the overall geometry and coordinates for the radar platform and the scene of interest which are used in this analysis. Section 3 presents the details of the Frank-coded transmission waveform that is applied in generation of the SAR images. Section 4 describes the methods used to compute the idealized impulse response of the target scene for each of the transmission waveforms within the synthetic aperture. Section 5 gives the techniques used to compute the simulated radar echoes that enter the receiver for each position along the synthetic aperture. Section 6 presents the convolution method used in the correlation receiver used to generate the SAR complex-valued radar data. Section 7 describes the details of the spotlight SAR image formation process used to generate the SAR imagery based upon the output of the correlation receiver. The conclusions are presented in the final section.

2. GEOMETRY AND COORDINATES

In order to analyze the potential applicability of Frank-coded LPI waveforms for SAR image formation, it is first necessary to define the coordinates corresponding to the radar platform and the scene to be imaged. Specifically, define $\{x, y, z\}$ to be a spatial Cartesian coordinate system. Here, the $z = 0$ coordinate surface defines the target ground plane with $\{x, y, z\} = \{0, 0, 0\}$. This coordinate origin is referred to as the ground reference point (GRP), and this location is the aim-point of the radar mainbeam for the spotlight SAR collection. The coordinate z increases with increasing elevation above the ground plane. The positive x coordinate is defined to correspond with increasing ground down-range from the radar. Finally, the y coordinate lies in the ground cross-range direction, so that $\{x, y, z\}$ forms a right-handed coordinate system.

The radar is modeled to transmit and receive a series of radar waveforms during a total time of T_0 along the entire synthetic aperture. Also, define t to be the slow-time coordinate for the mean time corresponding to the transmission and reception of a single radar waveform. Without loss in generality, define $t = 0$ to be the mid-point in time of the full synthetic aperture collection period. That, the slow-time t is assumed to vary between $-T_0/2$ and $T_0/2$ over the full synthetic aperture of the collection. Also, the ground down-range x coordinate lies along the projected line in the ground plane from the radar aperture center-point at $t = 0$ to the GRP. The ground cross-range coordinate y lies mutually perpendicular to the x and z coordinates. It is useful to consider the special case of an idealized point target within the ground plane of $z = 0$. Thus, the target is expressed in terms of the ground down-range and ground cross-range directions, x and y, respectively.

Next, it is useful to develop a parameterization of a radar platform trajectory corresponding to a straight and level flight path with constant speed and a broadside radar imaging geometry. One possible parameterization is the following in terms of a ground plane Cartesian coordinate system $\{x, y, z\}$:

$$X(t) = -X_0, \tag{1}$$

$$Y(t) = \pm V_0 t, \tag{2}$$

$$Z(t) = Z_0, \tag{3}$$

with V_0 equal to the speed of the radar platform, with X_0 equal to the radar ground range relative to the synthetic aperture center, and Z_0 equal to the radar elevation above the ground plane. Recall that the origin of the global Cartesian coordinates is selected to be the fixed aim-point on the ground to which the radar mainbeam is pointed

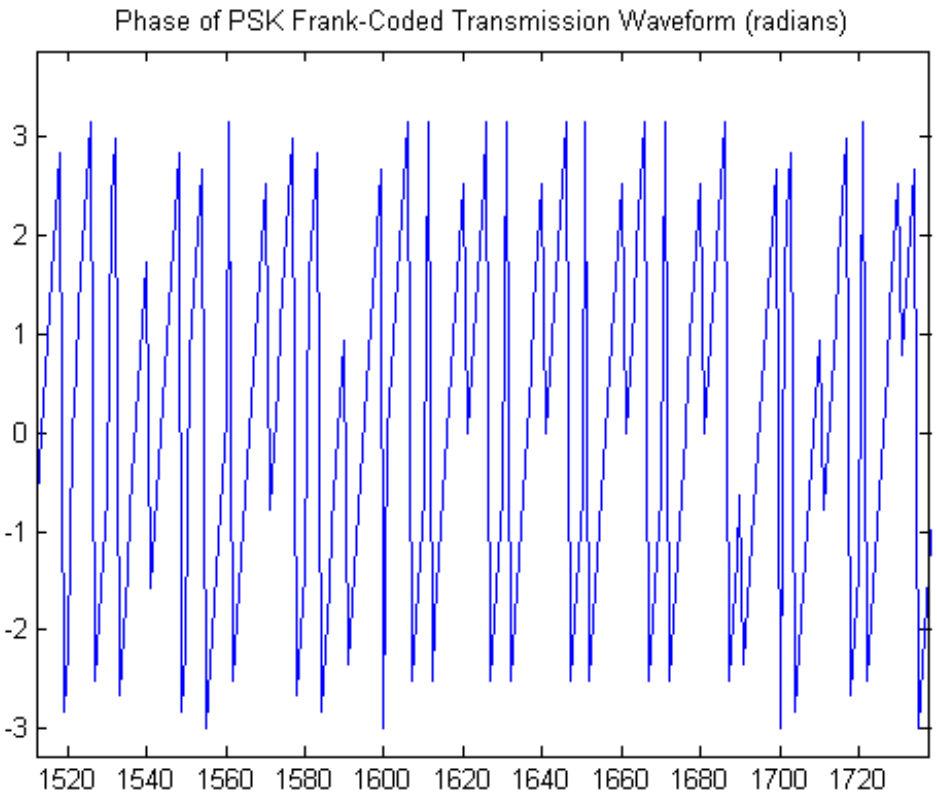

Figure 1. Phase of the Transmitted Frank-Coded Waveform

during this spotlight SAR image collection interval. This aim-point of the radar is also referred to as the GRP. The positive sign in (2) denotes radar motion in the $+y$ direction, and the minus sign defines movement in the $-y$ direction. From (1)-(3) above, the azimuth and elevation angles, respectively, of the radar platform relative to the GRP can be defined via:

$$\theta(t) \equiv \arctan\left(\frac{Y(t)}{X(t)}\right), \tag{4}$$

$$\varphi(t) \equiv \arctan\left(\frac{Z(t)}{\sqrt{X^2(t)+Y^2(t)}}\right). \tag{5}$$

3. TRANSMISSION RADAR WAVEFORM

The Frank code is a discrete-phase code that is based upon the fundamentals of linear frequency modulation. Specifically, the Frank code is obtained by taking the discrete phases of a linear chirp waveform via[2,7]

$$\omega_{i,k} \equiv \frac{2\pi}{M}\{i-1\}\{k-1\}, \;\; \{i=1,...,M\},\{k=1,...,M\} \tag{6}$$

with $N_c \equiv M^2$ equal to the pulse compression ratio. A plot of this waveform is provided in Figure 1 for the case of $M = 8$. The reciprocal of the constant time interval between phase changes, i.e., $1/\Delta t$, equals the approximate temporal bandwidth of the waveform.

Assume that the function $q(t)$ denotes the transmission waveform as a function of time t. The corresponding waveform in the spatial along-range r domain has the form:

$$p(r) \equiv q(t = 2r/c), \tag{7}$$

with c denoting the speed of light and the factor of 2 arising from the round-trip propagation of the waveform. It is convenient to select the zero position of the transmission waveform so that the mean waveform energy lies at the temporal value $t = 0$, corresponding to $r = 0$ in the spatial domain.

Define the ideal complex-valued radar reflectivity to be described by the function $f(x, y, z)$ at the scene GRP location where the radar mainbeam is pointed. This function mathematically describes the ideal complex-valued impulse response of the scene, which typically contains many variations of both specular and diffuse scattering objects. In reality, $f(x, y, z)$ can have some variation with regards to the observation angles θ and ϕ due to shadowing and related effects. However, such effects are expected to be relatively minor, especially at higher radar frequencies.

4. IDEALIZED RADAR ECHOES

To begin this analysis, it is necessary to generate the idealized impulse response of the scene corresponding to the radar sensor aspect and elevation angles for each radar waveform that is transmitted. The result of the ideal correlation processing is obtained by taking the convolution of the complex conjugate of the time-reversed transmitted waveform with the received radar echo from the scene location where the gain of the radar transmission beam is steered for that particular waveform. These idealized radar responses give the impulse response of the scene at the particular aspect and elevation angles of the radar sensor relative to the scene of interest.

The idealized radar echo is defined to be the reflected radar waveform formed from the complex superposition of the multiple scattering mechanisms within the spatial scene where the radar beam is steered, in the limit as the pulse width of the transmission waveform approaches zero. Of course, such an infinitely narrow pulse waveform uniformly excites all frequencies. That is, the idealized radar echo is the scattering response to a scene due to an infinitely sharp impulse transmission waveform.

Assume that there are some number of discrete radar scattering centers that are not shadowed to the radar at a given elevation angle θ and azimuthal angle ϕ describing the instantaneous radar sensor location relative to the scene center. Assume that each scattering center in the scene can be characterized by a complex-valued reflectivity σ and a location $\{x, y, z\}$ in the physical three-dimensional space within the scene of interest.

The idealized impulse of the projection range profile has the form:

$$\tilde{g}_{\theta,\phi}(\rho) = \int dx \int dy \int dz\, f(x, y, z)\, \delta\Big(x\cos(\theta)\cos(\phi) + y\cos(\theta)\sin(\phi) + z\sin(\theta) - s\Big). \tag{8}$$

This equation is basically a form of the 3-D Radon transform.[4,8]

In the simulation, a number of idealized point targets are inserted onto the ground plane in the approximate shape of a rectangle with a few additional points within the region. The corresponding idealized radar echo at the initial radar platform location along the synthetic aperture is shown in Figure 2

5. RECEIVED RADAR ECHOES

A computation of the resultant SAR imagery requires a calculation of the radar waveform that enters the receiver. Then, it is necessary to compute the correlation of the ideal scene response at this set of measurement aspect angles $\{\theta, \phi\}$ with the transmission waveform, i.e.,

$$g_{\theta,\phi}(s) = p(s) * \tilde{g}_{\theta,\phi}(s). \tag{9}$$

Thus, a Frank-coded radar waveform is transmitted and received at each set of measurement angles $\{\theta, \phi\}$ due to different values of the idealized received radar echo from the scene at each set of $\{\theta, \phi\}$.

As part of the spotlight SAR image formation process, the offset for the ideal received waveform is set so that an idealized point scattering center located at the ground reference point (GRP) $\{x, y\}$ corresponds to the value $s = 0$. For conventional SAR processing, the mean time of the transmission waveform $q(t) = p(ct/2)$, so that $s = 0$ corresponds to the mean time of the waveform $p(s)$ in the spatial domain.

The radar echo that enters the simulated radar receiver front-end, which is due to the radar reflections from the scene-of-interest, is shown in Figure 3

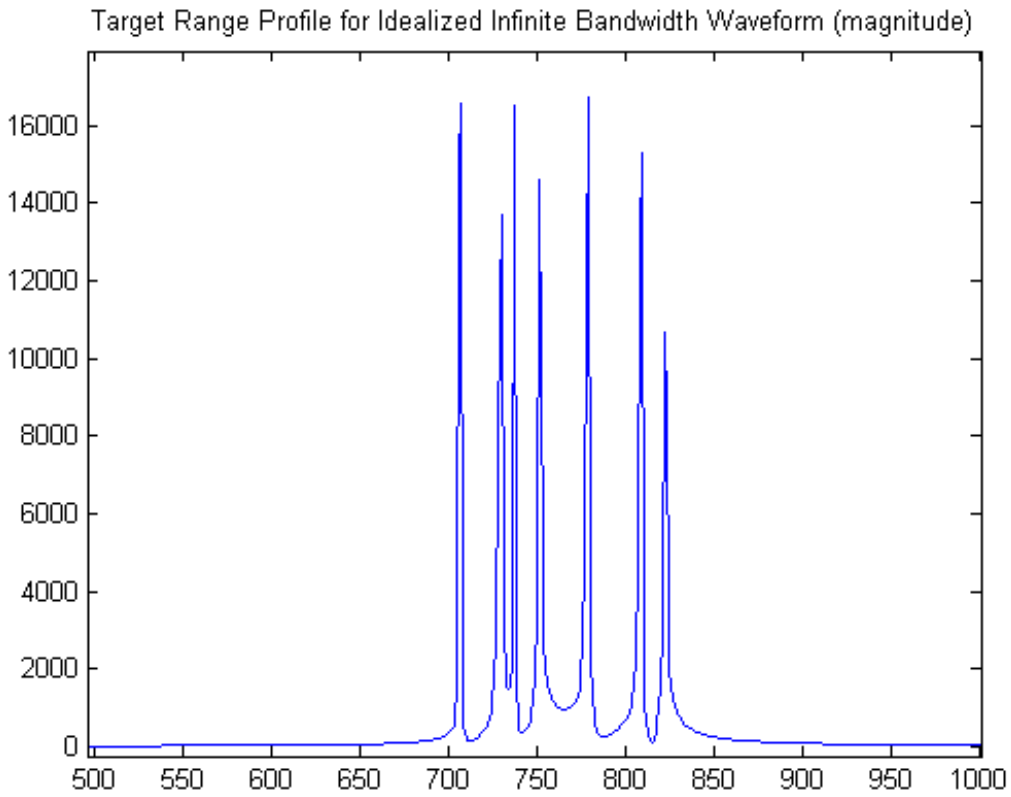

Figure 2. Idealized radar echo at the initial radar platform location along the synthetic aperture

6. CORRELATION RECEIVER PROCESSING

In order to model the receiver processing, the idealized radar echo for the interrogated scene at a relevant set of azimuthal and elevation angles is convolved with the selected Frank-coded radar waveform. The result of this correlation receiver processing is obtained by computing the convolution of the received waveform with the complex conjugate of the transmission waveform at the set of measurement angles under interrogation. This processing yields the range profile of the scene corresponding to each transmitted Frank-coded waveform along the synthetic aperture. This correlation processing dispreads the radar echoes that enter the receiver, so that range profiles are obtained from the scene consistent with the sidelobe properties of Frank waveforms. The resulting complex-valued range profiles enable the formation of resulting SAR imagery.

Specifically, it is necessary to compute the numerical result of the ideal correlation processing. This result is obtained by taking the convolution of the complex conjugate of the time-reversed transmitted waveform with the received radar echo from the scene location where the gain of the radar transmission mainbeam is steered for that particular waveform. For the receiver processing, the received radar echo function $g_{\theta,\phi}(s)$ is convolved with the radar waveform transmitted for the particular set of measurements angles $\{\theta, \phi\}$. The result of this correlation receiver processing is obtained by computing the convolution of the received waveform $g^*_{\theta,\phi}(s)$ with the complex conjugate of the spatially-reflected transmission waveform at the set of measurement angles under interrogation, i.e., $p^*_{\theta,\phi}(-s)$. This processing yields the range profile of the scene at the set of measurement angles $\{\theta, \phi\}$, i.e.,

$$h_{\theta,\phi}(s) = p^*_{\theta,\phi}(-s) * g_{\theta,\phi}(s). \tag{10}$$

The output of the simulated correlation receiver for one particular transmitted waveform along the synthetic aperture is shown in Figure 4

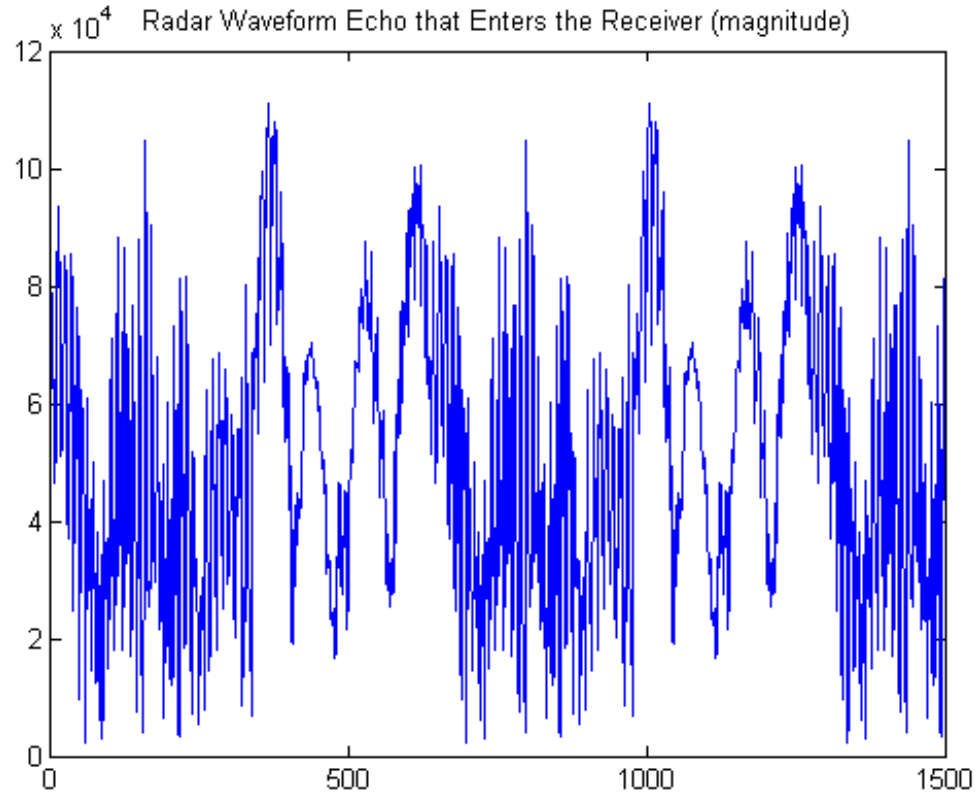

Figure 3. Radar echo due to the simulated Frank-coded waveform at the initial radar platform location along the synthetic aperture

7. IMAGE FORMATION

The correlation receiver yields the complex in-phase I and quadrature Q channels for each transmitted Frank-coded waveform along the synthetic aperture. These two channels are combined to give the complex phase history data for the SAR collection. Specifically, the complex magnitude of the two channels gives the magnitude, and the arctan of the ratio of Q over I yields the phase. These data are collected at the various frequencies $f_{m'}$ covered by the radar waveforms and at the different times t along the synthetic aperture. These signal processing operations yield the down-converted, frequency-domain SAR measurement data in the original "polar" format:

$$\tilde{G}(f_{m'}, t_{n'}) = \sum_i \sigma_i \exp(-j2\pi\Delta R_i(t_{n'})2f_{m'}/c). \tag{11}$$

In this equation, the path difference relative to the GRP is defined by

$$\Delta R_i(t_{n'}) \equiv R_i(\theta(t_{n'}), \varphi(t_{n'})) - R_0(\theta(t_{n'}), \varphi(t_{n'})). \tag{12}$$

Thus, this analysis gives the frequency domain SAR data based upon assumed geometries for the radar platform and the targets within the imaged scene. The polar-formatted frequency-domain data are related to the output of the correlation processor by a one-dimensional (1-D) Fourier transform along the range dimension.

In (11), the complex-valued measured quantities $\tilde{G}$ give both the real (i.e., in phase) and imaginary (i.e., quadrature) components of the sub-band centered on frequency sample value $f_{m'}$ corresponding to the Frank-coded radar waveform received at slow-time sample value $t_{n'}$. The constant c is the speed of light, and $j = \sqrt{-1}$ is the imaginary constant. The factor of 2 in the argument of the exponential function accounts for the two-way

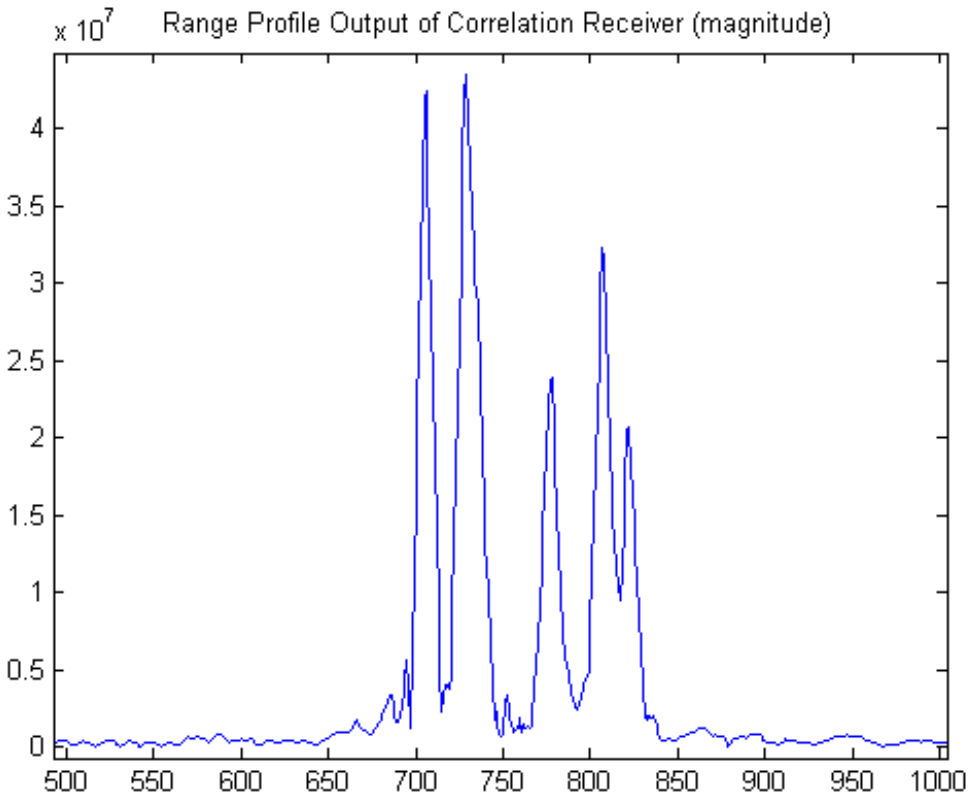

Figure 4. Output of the correlation receiver due to the simulated Frank-coded waveform at the initial radar platform location along the synthetic aperture

propagation of the radar. In (11), the summation over i applies to the multitude of scattering centers that can lie within the radar's footprint on the ground. In (12), the quantity $R_i(\theta(t_{n'}), \varphi(t_{n'}))$ is equal to the range or distance from the radar platform for the radar waveform received at slow-time $t_{n'}$ to the ith scattering center characterized by the complex-valued reflectivity σ_i:

$$R_i(\theta(t_{n'}), \varphi(t_{n'})) = \sqrt{\{X(t_{n'}) - \alpha(t_{n'})\}^2 + \{Y(t_{n'}) - \beta(t_{n'})\}^2 + \{Z(t_{n'})\}^2} \tag{13}$$

Likewise, $R_0(\theta(t_{n'}), \varphi(t_{n'}))$ equals the range from the radar platform to the spotlight SAR GRP lying at the $\{x, y, z\} = \{0, 0, 0\}$ coordinate origin, i.e.,

$$R_0(\theta(t_{n'}), \varphi(t_{n'})) = \sqrt{\{X(t_{n'})\}^2 + \{Y(t_{n'})\}^2 + \{Z(t_{n'})\}^2}. \tag{14}$$

The analysis of Frank-coded SAR-LPI concepts developed herein is applied specifically to spotlight SAR image data in the ground plane of $z = 0$. In order to obtain such ground plane image data, it is convenient to define the following functions for the ground range and the ground cross-range components of the spatial frequency, respectively,

$$\xi_m(f_{m'}, t_{n'}) \equiv \frac{2f_{m'}}{c} \cos(\theta(t_{n'})) \cos(\varphi(t_{n'})), \tag{15}$$

$$\eta_m(f_{m'}, t_{n'}) \equiv \frac{2f_{m'}}{c} \cos(\theta(t_{n'})) \sin(\varphi(t_{n'})). \tag{16}$$

Equations (15) and (16) are simply the direction cosine projections of the original polar sample data, with the spatial frequency spherical polar radius $2f'_m/c$, the azimuth angle $\theta(t_{n'})$, and the elevation angle $\phi(t_{n'})$.

A polar-to-rectangle sampling operation,[5] or a similar procedure, is applied to obtain the desired Cartesian-sampled data, i.e.,

$$\tilde{G}(f_{m'}, t_{n'}) \underset{\text{pol}}{\rightarrow} G(\xi_m, \eta_n). \tag{17}$$

Here, $G(\xi_m, \eta_n)$ denotes the complex-valued frequency-domain Cartesian data in terms of M discrete resampled values of the ground down-range spatial frequency ξ_m and N discrete resampled values of the ground cross-range spatial frequency η_n. From these data, a 2D discrete Fourier transform (DFT) yields the desired spotlight SAR image via:

$$G(\xi_m, \eta_n) \underset{\text{2D DFT}}{\longleftrightarrow} b(x_k, y_\ell). \tag{18}$$

In addition, it is assumed that both sensor motion compensation and autofocus processing have been applied previously to the data in order to obtain well- focused imagery of the stationary scene content.

The computation of the SAR images can be performed by evaluating the following expression:

$$b(x, y) = \int_{\xi_0 - \Delta\xi/2}^{\xi_0 + \Delta\xi/2} d\xi \int_{-\Delta\eta/2}^{\Delta\eta/2} d\eta \; \tilde{G}(\xi, \eta) \exp\left(j2\pi(x\xi + y\eta)\right) \tag{19}$$

with ξ_0 equal to the central value of the ground range spatial frequency.

The resultant SAR image formed using Frank-coded transmission waveforms is shown in Figure 5. The locations of the strong energy points within this image are consistent with the locations of the idealized point scattering centers that were inserted into the ground-plane. Thus, a successful SAR image was formed using Frank-coded transmission waveforms. Furthermore, Figure 5 indicates that the cross-range smearing is slightly more extended than the smearing in the down-range direction. Overall, the application of Frank-coded waveforms has yielded an excellent ability to reconstruct the ground scene remotely, while the use of Frank-coded waveforms conceptually allows this sensor to be LPI.

8. CONCLUSIONS

This paper has examined methods for using Frank-coded transmission waveforms for forming spotlight-mode SAR images. Simulations are developed based upon a matched correlation receiver corresponding to the transmitted Frank-modulated waveforms. This analysis demonstrates the ability to form SAR images via Frank-coded transmission and receiver processing, and that good reconstructions of the image scene can be obtained while using such a set of LPI waveforms.

Acknowledgment

DoD Distribution Statement A: Unlimited Distribution. The views expressed in this document are those of the authors and do not reflect the official policy or position of the Department of Defense or the U.S. Government.

REFERENCES

[1] W. G. Carrara, R. S. Goodman, and R. M. Majewski, "Spotlight Synthetic Aperture Radar Signal Processing Algorithms" Artech House, Norwood, MA 1995

[2] B. W. Gillespie and L. E. Atlas, "Optimizing time-frequency kernels for classification" IEEE Transactions on Signal Processing, Vol. 49, No. 3, pp. 485-496, March 2001.

[3] E. Giusti and M Martorella, Range Doppler and Image Autofocusing for FMCW Inverse Synthetic Aperture Radar IEEE Transactions on Aerospace and Electronic Systems, Volume 47, Issue 4, October 2011, pages 2807-2823.

[4] A. K. Jain, Fundamentals of Digital Image Processing", Prentice Hall, Englewood Cliffs, NJ, 1989.

[5] C. V. Jakowatz Jr., D. E. Wahl, P. H. Eichel, D. C. Ghiglia, and P. A.Thompson, "Spotlight-Mode Synthetic Aperture Radar: A Signal Processing Approach", Kluwer Academic, Norwell, MA, 1996.

[6] D. C. Munson, Jr., J. D. O'Brien and W. K. Jenkins, "A tomographic formulation of spotlight-mode synthetic aperture radar" Proceedings of the IEEE, Vol. 71, No. 8, pp. 917-925, 1983.

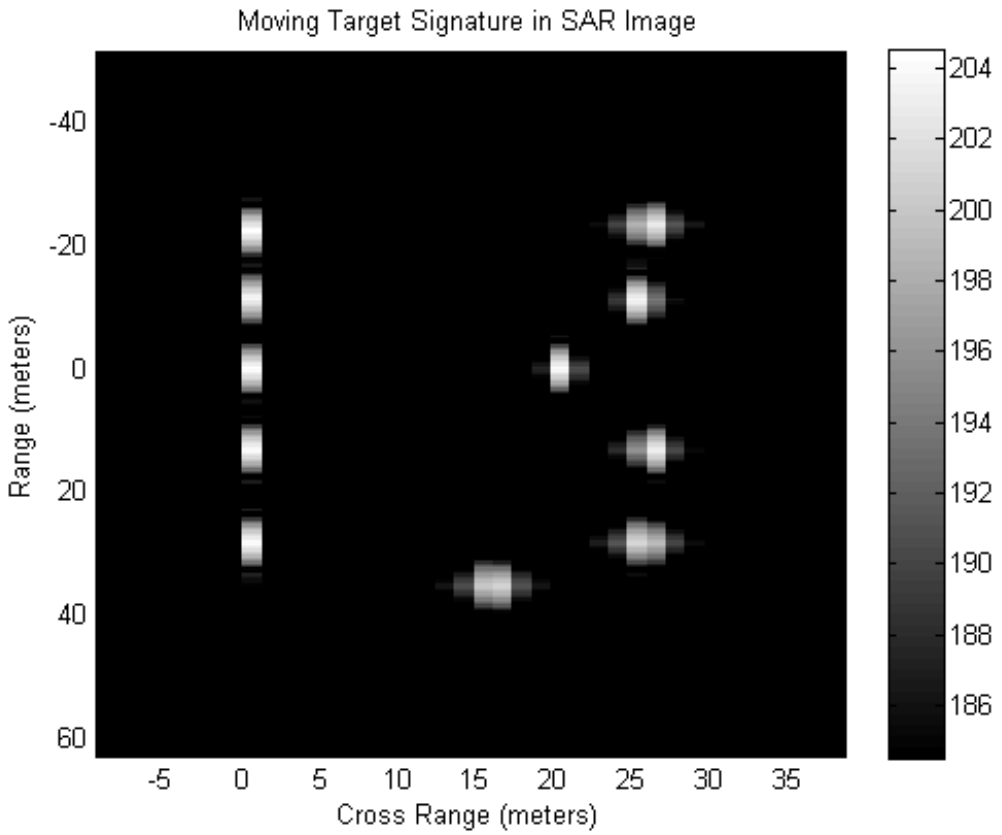

Figure 5. The resultant SAR image formed using Frank-coded transmission waveforms

[7] P. E. Pace, "Detecting and Classifying Low Probability of Intercept Radar" 2nd ed., Artech House, Boston, 2009.

[8] J. Radon, "Uber die Bestimmung von Funktionen durch ihre Integralwerte Tangs gewisser Mannigfaltikeiten (On the determination of functions from their integrals along certain manifolds)", Math. Phys. Klass, Vol. 69, pp. 262-277, 1917.

[9] J. L. H. Webb and D. C. Munson, Jr., "SAR image reconstruction for an arbitrary radar path" in 1995 International Conference on Acoustics, Speech, and Signal Processing in Detroit, MI, on 09-12 May 1995.

[10] S. Xiao and D. C. Munson, Jr., "Spotlight-mode SAR imaging of a three-dimensional scence using spectral estimation techniques", Geoscience and Remote Sensing Symposium Proceedings, 1998. IGARSS '98. 1998 IEEE International, Vol. 2, pp. 642-644.